

Electron Interference in a Double-Dopant Potential Structure

Josef Weinbub,* Mauro Ballicchia, and Mihail Nedjalkov

Herein, an analysis of interference effects as a result of the electron evolution within a coherent transport medium is presented, offering a double-dopant Coulomb potential structure. Injection of coherent electron states into the structure is used to investigate the effects on the current transport behavior within the quantum Wigner phase space picture. Quantum effects are outlined by using classical simulation results as a reference frame. The utilized signed particle approach inherently provides a seamless transition between the classical and quantum domain. Based on this the occurring quantum effects caused by the non-locality of the action of the quantum potential, leading to spatial resonance, can be identified. The resulting interference patterns enable novel applications in the area of entangletronics.


Introduction: Correctly describing and predicting quantum effects in nanoelectronic devices remains a key challenge. An attractive way to do so is to compare quantum with classical effects, enabling to identify quantumness in the generated results. However, the transition from quantum to classical transport requires a principal change in the physical description.

In contrast to classical processes comprised by elementary events associated with probabilities, the interplay of phases and amplitudes gives rise to interference effects which cannot be described as a cumulative sum of probabilities. A given quantum transport problem does not allow for a decomposition into separate sub-tasks as suggested by the Matthiessen rule of classical transport, and needs to be treated in its entirety.^[1] Therefore, the interplay of seemingly simple processes, as for example electron evolution with Coulomb potentials, fundamentally differs when using a classical or a quantum description.

Dr. J. Weinbub
Christian Doppler Laboratory for High Performance TCAD
Institute for Microelectronics
TU Wien, Austria
E-mail: josef.weinbub@tuwien.ac.at

Dr. M. Ballicchia, Prof. M. Nedjalkov
Institute for Microelectronics
TU Wien, Austria

Dr. M. Ballicchia
Department of Information Engineering
Università Politecnica delle Marche
Italy

 The ORCID identification number(s) for the author(s) of this article can be found under <https://doi.org/10.1002/pssr.201800111>.

© 2018 The Authors. Published by WILEY-VCH Verlag GmbH & Co. KGaA, Weinheim. This is an open access article under the terms of the Creative Commons Attribution License, which permits use, distribution and reproduction in any medium, provided the original work is properly cited.

DOI: 10.1002/pssr.201800111

A convenient approach to implement a seamless transition between classical and quantum descriptions is offered by the Wigner transport model, based on the Wigner function^[2] and implemented by a signed particle approach^[3]: The Wigner approach can be reduced to the Boltzmann transport model, when the quantum rules for particle evolution are replaced by classical ones. In the classical case the evolution is governed by the local force (the first derivative of the potential). However, in the quantum case all derivatives of the potential control the evolution, as can be seen on the right-hand side of the expansion of the ballistic Wigner equation^[4]:

$$\frac{\partial f_w}{\partial t} + \frac{\bar{p}}{m} \nabla f_w + \vec{F}(\vec{r}) \nabla \bar{p} f_w = - \left(\frac{\hbar}{2}\right)^2 \frac{1}{3!} \frac{\partial^3 V(\vec{r})}{\partial \vec{r}^3} \frac{\partial^3 f_w}{\partial \vec{p}^3} + \dots \quad (1)$$

This approach gives rise to non-local and tunneling effects which both can be conveniently studied by means of simulation. As a consequence, it naturally enables switching between classical and quantum transport in a flexible and straightforward manner using the same modeling and simulation backend. Based on this, the role of physical conditions can be investigated in detail, such as investigating the electron evolution within a specific transport medium.

It has been demonstrated that the concepts of coherence and entanglement are quantitatively equivalent.^[5] Entanglement is the term of choice for nanoelectronic problems, where a system called device is open to its environment through a system called contacts. In this work the term entanglement is thus understood to represent the complicated coupling between device and contact states. It further covers the term entangletronics,^[6] short for entangled electronics, and extends it over a much broader class of problems beyond the strict meaning of quantum entanglement. Therefore, entangletronics is understood to rely on mechanisms which maintain coherence, while the environment strives to destroy it.

In a previous communication we showed that the Wigner formalism provides a legitimate theoretical framework for presenting the basic notions of the quantification theory of coherence in phase space terms.^[6] Based on the resulting criteria for coherence in phase space in conjunction with a Wigner signed particle approach, we demonstrated that a quantum state can be split and controlled by an electrostatic lense and how the environment kills the coherence.

Here we report a new advancement, also paving the way for building novel entangletronic devices. Based on ViennaWD^[7]

and its Wigner signed particle approach, recently supporting switching between quantum and classical transport, we analyze the current transport behavior with two attractive, that is, pulling, dopants (modeled via Coulomb potentials) in a transport medium.

The motivation behind investigating the effects of dopants in a transport medium is that they can be introduced on purpose in a controlled manner by fabrication processes. This enables to specifically design the current transport path down to the nanometer regime.^[8,9]

Concerning transport properties, we assume ballistic transport, which in terms of wave mechanics relates to coherent transport: In the used quantum transport model (used for simulating nanoelectronic devices), coherence is destroyed by any process which influences the free movement of the signed particles, for example, phonon scattering. Although the theory and the simulation framework support phonon scattering,^[6] here our focus is on clearly highlighting the manifesting quantum effects. This requires a maximum resolution of the results, in turn requiring that all phonon scattering effects are suppressed. To enable coherent evolution, the injected electrons must be coherent in the first place. Therefore, we continuously inject coherent minimum uncertainty wave packets and let them collide with the dopants. The observed spatial resonance behavior is particularly attractive for applications in entangletronics.

The findings provide valuable insights into the yet not fully understood physics of the transition from quantum to classical behavior. Even more so, a direct comparison between the classical and the quantum simulation results enables to clearly identify the quantum effects occurring in quantum dynamics experiments with dopants.

The contributions of this work are primarily twofold: 1) We investigate the impact of an attractive double-dopant setup on electron evolution, and 2) we highlight the current transport inherent quantum effects by comparing classical with quantum transport simulations.

Experimental Setup: The simulation domain has the extent of $40 \times 60 \text{ nm}^2$, with absorbing boundary conditions. The attractive dopants are modeled via Coulomb potentials (peak potential 0.365 eV) and are placed at $y = 30 \text{ nm}$ and $x = 14 \text{ nm}$ and $x = 26 \text{ nm}$, respectively. In the quantum case the identical injected states are Wigner functions corresponding to minimum uncertainty wave packets^[10] (representing electrons), which are described by Wigner pure states:

$$f_{\text{W}}(\bar{r}, \bar{k}) = N \exp\{-|\bar{r} - \bar{r}_0|^2 / (2\sigma^2)\} \exp\{-|\bar{k} - \bar{k}_0|^2 / 2\sigma^2\} \quad (2)$$

The initial Gaussian-shaped envelope of plane waves (Gaussian function in both position and momentum) has thus the ability to form interference patterns. These electron states are injected at $r_{0,x} = 20 \text{ nm}$, $r_{0,y} = 0 \text{ nm}$ (period 1 fs, direction $+y$, initial kinetic energy 0.141 eV, $5 \cdot 10^5$ signed particles per state), using a spatial standard deviation of $\sigma_x = \sigma_y = \sigma = 16 \text{ nm}$ for the Gaussian, corresponding to the equilibrium distribution around $k_{0,x} = 0$, $k_{0,y} = 16\Delta k$ with the effective mass $m^* = 0.19m_{\text{electron}}$

at a temperature of $T = 300 \text{ K}$. The square mesh in the momentum space ($\Delta k = \pi/L_c$) is determined by the coherence length $L_{c;x,y} = 60 \text{ nm}$. The coherence length has been set to the largest extension of the simulation domain, that is 60 nm, in order to have coherent transport inside the simulation domain, and corresponds to an energy of $\hbar^2 \Delta k^2 / (2m^*) = 0.55 \text{ meV}$. To enable a coherent evolution, the Wigner pure states must be injected with a constant σ : Injection of mixed states, for example, according to Fermi-Dirac or Maxwell-Boltzmann distributions, already introduces decoherence in ballistic devices.^[11] Thus, in the case of coherent injection, σ does not vary according to a given distribution, but is kept constant.

The quantum states can be interpreted as distributions of classical electrons, so that apart from normalization problems we can safely ensure equivalent injecting conditions for both, the classical and the quantum experiments. Classical and incoherent perceptions become synonyms; a loss of coherence is equivalent to a transition to classical behavior. In coherent problems, the classical and the quantum experiment differ in the treatment of the dopant potentials. In the classical case, the first derivatives of the potential give rise to a force and acceleration along Newtonian trajectories, while in the quantum case higher order derivatives are taken into account via the Wigner potential, cf. right-hand side of (1). The latter enables describing quantum effects, e.g., non-locality.

Analysis: Figure 1 and Figure 2 show the electron density at 200 fs for all absorbing boundary conditions in the classical and in the quantum case, respectively. Steady-state is reached after 160 fs. The green isolines indicate the potential energy of the

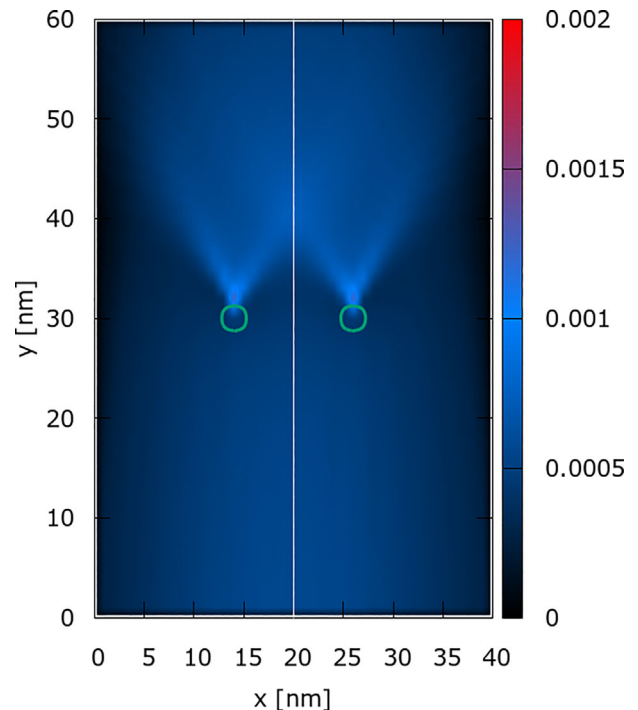


Figure 1. Classical electron density ([a.u.]) after 200 fs of the initial minimum uncertainty condition. The green circles are isolines at 0.175 eV of the Coulomb potentials modeling the dopants.

¹ <http://viennawd.sourceforge.net/>

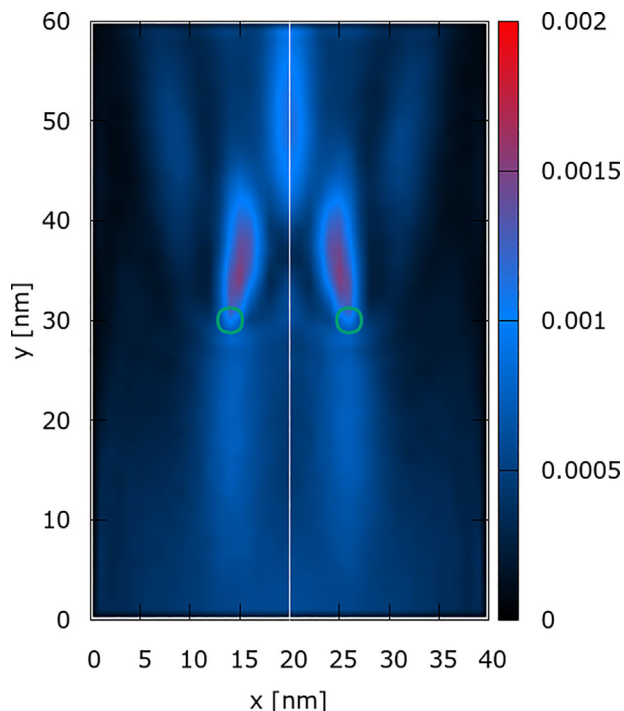


Figure 2. Quantum electron density ([a.u.]) after 200 fs of the initial minimum uncertainty condition. The green circles are isolines at 0.175 eV of the Coulomb potentials modeling the dopants.

dopants at 0.175 eV, which is approximately half of the peak energy level of the dopants.

In the classical case, Figure 1, no interference pattern can be recognized beyond the dopants ($y > 30$ nm) as the action of the electric force is local. Thus, for $y < 30$ nm, the density, after reaching the steady-state, is similar to the case of a freely evolving initial condition (i.e., the injected states). The effect of the two potentials is, however, noticeable behind the dopants. Right behind each dopant, the symmetry of the density distribution reflects the symmetry of the Coulomb force. Until approximately $y = 40$ nm, correlation effects in the density are observed, caused by the

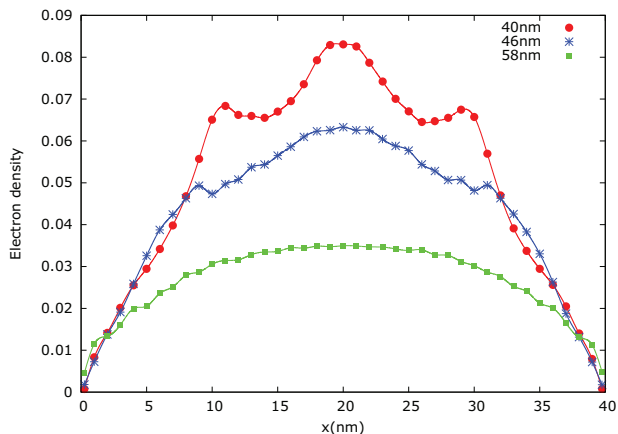


Figure 3. Classical screens show the cumulative density ([a.u.]) recorded at three different y positions.

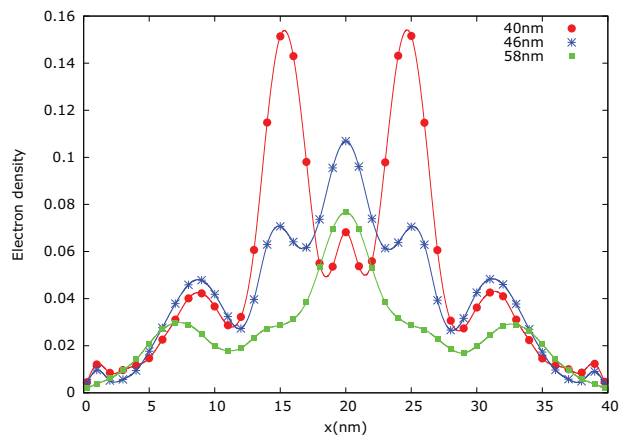


Figure 4. Quantum screens show the cumulative density ([a.u.]) recorded at three different y positions.

accumulation of electrons due to the modification of the trajectories which are in turn caused by the force. This manifests in the three peaks at the 40 nm screen shown in **Figure 3**. For $y > 40$ nm, the correlation rapidly fades away within a 10 nm distance.

In the quantum case, Figure 2, the non-locality action of the quantum potential of the dopants affects the injected electrons right after injection². For $y < 30$ nm, the density follows the symmetry of the individual Coulomb potentials. The situation changes dramatically in the upper half ($y > 30$ nm), showing a complicated picture of spatial resonances. These do not fade away as in the classical case, but maintain the peak pattern which evolves with the distance (**Figure 4**). The simple quantum effect of non-locality already significantly influences the physical behavior of the electron. The sensitivity of the effect is manifested in the change of the pattern with the distance from the dopants. Therefore, even a small change of the potential of one of the dopants (e.g., peak energy, profile) will cause a dramatic change in the pattern. All in all, the spatial resonance as well as their correlation with the dopant potentials enable to selectively manipulate the electron evolution, which, as already indicated, is attractive for future applications in entangletronics.

However, it is important to note that the evolving peaks cannot be considered as individual electrons which advance in the phase space in an eventually entangled way. The pure state evolution is time reversible so that if one of the peaks is evolved backwards to the time origin, it will become a subset of the original minimum uncertainty wave packet (2). Therefore, a single evolving peak cannot be the result of a single electron.

The results bear a resemblance to the diffraction patterns manifesting over time in double-slit experiments.^[12–14] However, there is a fundamental difference: With the double-slit experiments, the classical behavior is a reflection at the barrier, where in the quantum case, tunneling effects occur. In our case, only non-locality effects are experienced as the dopants do not act as a barrier. Therefore, no tunneling effects appear.

Another interesting advantage of our simulation approach is the fact, that we are able to use an arbitrary number of screens behind each other within a single experiment. The screens are

²This is already expected in the case of a single dopant.

not physical detectors: There is no physical interaction with the system. Therefore, we do not lose the coherence of the wave function upon recording the position of the signed numerical particles. On the contrary, conventional screen experiments (for instance used in double-slit experiments) suffer from a loss of coherence (the wave-function collapses) upon measuring the position.

Summary: We reported the quantum simulation of interference effects of a double-dopant Coulomb potential structure. The utilized Wigner signed particle approach provides a convenient and natural way of seamlessly switching between the classical and quantum domain. We discussed the impact of the dopant setup on the electron evolution, highlighted the quantum effects, compared to classical simulations, and underlined the method's unique ability to place multiple detection screens. In conclusion, we stress that the discussed effects occur at small scales, so that even small changes of the physical conditions can affect them. The study of the arising quantum effects is important on a fundamental level for gaining insights into the not-well-explored area of quantum transport phenomena for developing novel principles of device operation within the scope of entangletronics.

Acknowledgements

The financial support by the Austrian Science Fund (FWF; Austria) project FWF-P29406-N30, the Austrian Federal Ministry of Science, Research and Economy, and the National Foundation for Research, Technology and Development is gratefully acknowledged. The computational results presented have been achieved using the Vienna Scientific Cluster (VSC).

Conflict of Interest

The authors declare no conflict of interest.

Keywords

double-dopants, electron interference, entangletronics, quantum dynamics, wigner signed particle approach

Received: March 8, 2018

Revised: April 2, 2018

Published online: April 30, 2018

- [1] D. K. Ferry, *Semiconductor Transport*, Taylor & Francis, London, UK **2000**.
- [2] E. Wigner, *Phys. Rev.* **1932**, *40*, 749.
- [3] M. Nedjalkov, D. Querlioz, P. Dollfus, H. Kosina, *Wigner Function Approach*, Springer, New York, USA **2011**, pp. 289.
- [4] M. Nedjalkov, S. Selberherr, D. K. Ferry, D. Vasileska, P. Dollfus, D. Querlioz, I. Dimov, P. Schwaha, *Ann. Phys.* **2013**, *328*, 220.
- [5] A. Streltsov, U. Singh, H. S. Dhar, M. N. Bera, G. Adesso, *Phys. Rev. Lett.* **2015**, *115*, 020403.
- [6] P. Ellinghaus, J. Weinbub, M. Nedjalkov, S. Selberherr, *Phys. Status Solidi RRL* **2017**, *11*, 1700102.
- [7] P. Ellinghaus, J. Weinbub, M. Nedjalkov, S. Selberherr, I. Dimov, *J. Comput. Electron.* **2015**, *14*, 151.
- [8] M. Rashidi, J. A. Burgess, M. Taucer, R. Achal, J. L. Pitters, S. Loth, R. A. Wolkow, *Nat. Commun.* **2016**, *7*, 13258.
- [9] B. Fresch, J. Bocquel, D. Hiluf, S. Rogge, R. D. Levine, F. Remacle, *Chem. Phys. Chem.* **2017**, *18*, 1790.
- [10] D. Querlioz, P. Dollfus, *The Wigner Monte Carlo Method for Nanoelectronic Devices*, ISTE, London, UK; Wiley, Hoboken, USA **2010**.
- [11] I. Knezevic, *Phys. Rev. B* **2008**, *77*, 125301.
- [12] A. Tonomura, J. Endo, T. Matsuda, T. Kawasaki, H. Ezawa, *Am. J. Phys.* **1989**, *57*, 117.
- [13] O. Nairz, M. Arndt, A. Zeilinger, *Am. J. Phys.* **2003**, *71*, 319.
- [14] R. Bach, D. Pope, S. H. Liou, H. Batelaan, *New J. Phys.* **2013**, *15*, 033018.